Efficient Conservative Second-Order Central-Upwind Schemes for Option Pricing Problems

Omishwary Bhatoo*1, Arshad Ahmud Iqbal Peer †2, Eitan Tadmor ‡3, Désiré Yannick Tangman §4, and Aslam Aly El Faidal Saib ¶5

1,2,5Department of Applied Mathematical Sciences, University of Technology, Mauritius, La Tour Koenig, Pointe-aux-Sables 11134, Mauritius
3Department of Mathematics, Institute for Physical Sciences and Technology (IPST) and Center of Scientific Computation and Mathematical Modeling (CSCAMM) University of Maryland, College Park, MD 20742- 4015, USA
4Department of Mathematics, University of Mauritius, Réduit 80837, Mauritius

Abstract: The conservative Kurganov-Tadmor (KT) scheme was successfully applied to option pricing problems by Ramírez-Espinoza and Ehrhardt [Adv. Appl. Math. Mech. 5 (2013), pp. 759-790]. This included the valuation of European, Asian and non-linear options as Black-Scholes PDEs, written in the conservative form, by simply updating fluxes in the "Black-Box" approach. In this paper, we describe an improvement of this idea through fully vectorised algorithm of non-oscillatory slope limiters and efficient use of time solvers. Also, we propose the application of second-order extensions of KT to option pricing problems. Our test problems solve one-dimensional benchmark and convection-dominated European options as well as digital and butterfly options. This demonstrates the robustness and flexibility of the pricing methods and sets a basis for complex problems. Further, computation of option Greeks ensures reliability of the methods. Numerical experiments are performed on barrier options, early exercisable American options and two-dimensional fixed and floating strike Asian options. To the authors' knowledge, this is the first time American options are priced by applying the early exercise condition on the semi-discrete formulation of central-upwind schemes. Results show second-order, non-oscillatory and high-resolution properties of the schemes as well as computational efficiency.

Keywords: Black-Scholes PDEs; central-upwind schemes; non-oscillatory reconstructions; American options; Asian options; barrier options

1 Introduction

The famous Black-Scholes model prices different types of options. However, unlike European options, no analytical solution exists for many options including American, Asian and non-linear problems. Amongst several proposed numerical approaches, popular ones include Tangman et al. (2008) for American options and Oosterlee et al. (2004) for Asian options. However, similar to these approaches many others are customised to price only specific type of options. Over the last decades, numerical methods originally developed for hyperbolic conservation laws, have been applied to option pricing problems. These includes Oosterlee et al. (2004), Lötstedt and von Sydow (2015) and Ramírez-Espinoza and Ehrhardt (2013).

Ramírez-Espinoza and Ehrhardt (2013) applied the second-order central-upwind semi-discrete scheme of Kurganov and Tadmor (2000), denoted as KT, to price European, Asian and non-linear options. This approach avails of the "Black-Box" property of KT; it requires no Riemann solver and characteristic decomposition. This allows pricing options under Black-Scholes PDEs in the conservative form by sufficiently changing fluxes, initial and boundary conditions. The central-upwind nature guarantees smaller

---

*Email: obhatoo@umail.utm.ac.mu

†Corresponding author. Email: apeer@umail.utm.ac.mu

‡Email: tadmor@cscamm.umd.edu

§Email: y.tangman@uom.ac.mu

¶Email: asaib@umail.utm.ac.mu

numerical dissipation than fully central schemes through accurate estimates of Riemann fans. Further, the semi-discrete property offers numerical viscosity independent of $\mathcal{O}(1/\Delta t)$ for time-step Δt. Based on these properties and owing to the use of slope limiters, non-oscillatory and high-resolution solutions are achieved. However, as discussed in Ramírez-Espinoza (2011), the Asian option pricing problems suffered from intensive computation and heavy time consumption due to execution of heavily nested loops underlying the selected slope limiter.

In this paper, we first describe the KT algorithm in a fully vectorised setup to ensure computational efficiency; this bypasses heavily nested loops of slope limiters. Several slope limiters and time solvers are studied and best suited ones are employed. Our numerical experiments approximate option prices and Greeks namely delta and gamma. Other than European and Asian options, we extend the "Black-Box" approach to price digital, butterfly, American and barrier options by updating fluxes, initial and boundary conditions. We price American and barrier options by effortlessly modifying the algorithm's semi-discrete spatial reconstruction, which to the authors' knowledge, is a first; modifications include incorporating the early exercising condition for American options and imposing the barrier level for barrier options. Also, we discuss the second-order extensions of Kurganov and Tadmor (2000) by Kurganov et al. (2001) and Kurganov and Lin (2007) applied to option pricing.

This paper is organised as follows. In Section 2, we present an overview of option preliminaries and the backward-in-time Black-Scholes PDEs. Next, Section 3 describes the second-order KT reconstruction and its extensions as well as the forward-in-time Black-Scholes PDEs written in the conservative form. Non-oscillatory slope limiters and stable time methods are discussed in Section 4. Based on proposed improvements and the "Black-Box" framework, Section 5 describes numerical experiments which are performed on a series of options namely European, American, barrier, butterfly, digital and Asian.

2 Option Preliminaries and Black-Scholes Pricing Model

An option refers to the financial agreement between a writer and a holder. It locks a future possible transaction of a predetermined underlying asset s, at a predefined strike price K, and maturity date T, where $0 \leq t \leq T$. At the inception of an option life, no exchange of financial asset occurs; the option holder instead earns the right but not the obligation to buy or sell the underlying prior to or at maturity against the upfront option value paid to the writer. Option valuation is complex and its difficulties accrue with increasing option styles which depend mostly on exercising techniques, payoff profiles, path dependency of payoffs and trading strategies/combinations.

Amongst the wide variety of options traded on the market, we consider some commonly discussed models. Standard European options are exercisable only at maturity. American options are difficult to price as they can be exercised at any instant prior to or at expiry. Both option styles feature identical payoff profile illustrating the profit/loss graphically over the option life. As for exotic options, they have complex structures. The payoff of Asian options depends on the average underlying price over a predetermined time period and digital options pay a fixed amount or the value of the underlying security after the underlying stock exceeds the predetermined strike price. Other option pricing challenges arise from non-smoothness, sharp discontinuities or kinks appearing in payoff and Greek profiles, which are common to digital options and butterfly spread.

We price options under the Black-Scholes model by Black and Scholes (1973) and Merton (1973), which boils down to the backward-in-time parabolic PDE,

$$\frac{\partial v}{\partial t} + \frac{1}{2}\sigma^2 s^2 \frac{\partial^2 v}{\partial s^2} + (r - \delta)s\frac{\partial v}{\partial s} - rv = 0, \tag{1}$$

with risk-free interest rate r, constant volatility σ, time $t \in [0, T]$ and option price $v := v(s, t)$. The price process $\{s\}_{t \geq 0}$ where $s := s(t)$ and $s \in [s_{\min}, s_{\max}]$, follows the stochastic differential equation $\mathrm{d}s = (r - \delta)\,\mathrm{d}t + \sigma s\,\mathrm{d}W$ under the risk neutral measure, with continuous dividend yield, δ and Wiener process, W. The benchmark model (1) is used to test numerical methods subject to payoff function $v(s, T)$ and boundary conditions $BC_1(t) := v(s_{\min}, t)$ and $BC_2(t) := v(s_{\max}, t)$, for all t. PDE (1) principally governs European calls and puts options subject to terminal conditions,

$$v(s, T) = \max(s - K, 0) \text{ for call} \quad \text{and} \quad v(s, T) = \max(K - s, 0) \text{ for put}, \tag{2}$$

and boundary conditions for

$$\text{call} \quad \begin{cases} v(s, t) &= 0 \quad \text{as} \quad s \to 0, \\ v(s, t) &= s \exp\left(-\delta(T - t)\right) - K \exp\left(-r(T - t)\right) \quad \text{as} \quad s \to \infty, \end{cases}$$

$$\text{put} \quad \begin{cases} v(s, t) &= K \exp\left(-r(T - t)\right) - s \exp\left(-\delta(T - t)\right) \quad \text{as} \quad s \to 0, \\ v(s, t) &= 0 \quad \text{as} \quad s \to \infty. \end{cases} \tag{3}$$

For American options with the early exercise feature, PDE (1) is transformed into the inequality

$$\frac{\partial v}{\partial t} + \frac{1}{2}\sigma^2 s^2 \frac{\partial^2 v}{\partial s^2} + (r - \delta)s\frac{\partial v}{\partial s} - rv \leq 0, \tag{4}$$

with boundary conditions for

$$\text{call} \quad \begin{cases} v(s, t) &= 0 \quad \text{as} \quad s \to 0, \\ v(s, t) &= s - K \quad \text{as} \quad s \to \infty, \end{cases} \qquad \text{put} \quad \begin{cases} v(s, t) &= K - s \quad \text{as} \quad s \to 0, \\ v(s, t) &= 0 \quad \text{as} \quad s \to \infty, \end{cases} \tag{5}$$

No efficient analytical solution exists for (4), therefore numerical approaches solve (1) with the appropriate early exercise constraint imposed at each time level over the option life $0 \leq t \leq T$,

$$v(s, t) \geq \max(s - K, 0) \text{ for call} \quad \text{and} \quad v(s, t) \geq \max(K - s, 0) \text{ for put.} \tag{6}$$

The exotic path-dependent Asian options rely on the continuous arithmetic average $a := a(t)$ of the asset price s over $[0, t]$, where $a := \frac{1}{t}\int_0^t s(\tau)\,d\tau$. Asian options conform to no closed form solution. Arithmetic Asian options are of types fixed or floating strike. Fixed Asian options have a specified strike and floating Asian options have a strike equivalent to the average of the underlying asset over the option life. For Asian options' price $v := v(s, a, t)$, Barraquand and Pudet (1996) modified (1) for non-dividend paying asset price s to formulate a PDE defined in two spatial variables s and a,

$$\frac{\partial v}{\partial t} + \frac{1}{2}\sigma^2 s^2 \frac{\partial^2 v}{\partial s^2} + rs\frac{\partial v}{\partial s} - rv + \frac{1}{t}(s - a)\frac{\partial v}{\partial a} = 0, \tag{7}$$

subject to terminal payoffs $v(s, a, T)$ for

$$\text{call} \quad \begin{cases} \max(a - K, 0) & \text{fixed strike,} \\ \max(s - a, 0) & \text{floating strike,} \end{cases} \qquad \text{put} \quad \begin{cases} \max(K - a, 0) & \text{fixed strike,} \\ \max(a - s, 0) & \text{floating strike,} \end{cases} \tag{8}$$

and boundary conditions

$$\begin{aligned} \frac{\partial v}{\partial t} - \frac{a}{t}\frac{\partial v}{\partial a} - rv &= 0, \quad \text{as} \quad s \to 0, \\ \frac{\partial v}{\partial t} + \frac{1}{t}(s - a)\frac{\partial v}{\partial a} &= 0, \quad \text{as} \quad s \to \infty. \end{aligned} \tag{9}$$

PDE (7) is convectively dominated due to the absence of diffusion term in a-direction (Zvan et al., 1998).

3 Second-Order Central-Upwind Reconstructions

We consider the second-order cental-upwind semi-discrete KT scheme (Kurganov and Tadmor, 2000). It originally solves the hyperbolic conservation laws,

$$\frac{\partial v}{\partial t} + \frac{\partial}{\partial s}F(v) = 0, \tag{10}$$

with spatial variable s, conserved quantity v and convection flux F. We overview the KT scheme with uniform spatial grid points $\{s_j\}_{j=0}^N$ for $N \in \mathbb{N}$, width Δs and mid-cells $[s_{j-\frac{1}{2}}, s_{j+\frac{1}{2}}]$ where $s_{j\pm\frac{1}{2}} :=$

$s_j \pm \frac{\Delta s}{2}$. We let $\Delta t^n := t^{n+1} - t^n$ and define $v(s_j, t^n)$ and v_j^n respectively as the exact and approximate solution at point (s_j, t^n). It is assumed that previously computed cell-averages $\{\bar{v}_j\}$ at t^n are available,

$$\bar{v}_j^n \approx \bar{v}(s_j, t^n) := \frac{1}{\Delta s} \int_{s_{j-\frac{1}{2}}}^{s_{j+\frac{1}{2}}} v(s, t^n) \, \mathrm{d}s.$$

• **Reconstruction Step:** Next, based on cell-averages $\{\bar{v}_j\}$, a linear piecewise interpolant is constructed,

$$\tilde{v}_j^n \approx \tilde{v}(s_j, t^n) := \sum_j \left[\bar{v}_j^n + (v_s)_j^n (s - s_j) \right] \chi_{[s_{j-\frac{1}{2}}, s_{j+\frac{1}{2}}]}, \tag{11}$$

with characteristic function χ and spatial derivatives $(v_s)_j^n := v_s(s_j, t^n)$. Approximation of $(v_s)_j^n$ using the θ-dependent minmod (MM) limiter (Kurganov and Tadmor, 2000) guarantees non-oscillatory solution,

$$(v_s)_j := \mathrm{MM} \left(\theta \frac{\bar{v}_j - \bar{v}_{j-1}}{\Delta s}, \; \frac{\bar{v}_{j+1} - \bar{v}_{j-1}}{2\Delta s}, \; \theta \frac{\bar{v}_{j+1} - \bar{v}_j}{\Delta s} \right), \tag{12}$$

$$\text{where} \quad 1 \leq \theta \leq 2 \quad \text{and} \quad \mathrm{MM}(z_1, z_2, \ldots) = \begin{cases} \min_j(z_j), & \text{if} \quad z_j > 0 \quad \forall j, \\ \max_j(z_j), & \text{if} \quad z_j < 0 \quad \forall j, \\ 0, & \text{otherwise.} \end{cases}$$

• **Evolution Step:** At the upper cell boundaries $s_{j+\frac{1}{2}}$, the local speed of wave propagation is given by

$$c_{j+\frac{1}{2}}^n := \max \left(\left| \frac{\partial F}{\partial v} \left(v_{j+\frac{1}{2}}^- \right) \right|, \; \left| \frac{\partial F}{\partial v} \left(v_{j+\frac{1}{2}}^+ \right) \right| \right), \tag{13}$$

$$\text{where} \quad v_{j+\frac{1}{2}}^+ := \bar{v}_{j+1}^n - \frac{\Delta s}{2} (v_s)_{j+1}^n \quad \text{and} \quad v_{j+\frac{1}{2}}^- := \bar{v}_j^n + \frac{\Delta s}{2} (v_s)_j^n, \tag{14}$$

denote the respective left and right intermediate values of $\tilde{v}(s, t^n)$ at $s_{j+\frac{1}{2}}$. Use of finite speed of propagation separates between non-smooth $[s_{j+\frac{1}{2}, l}^n, s_{j+\frac{1}{2}, r}^n]$ and smooth $[s_{j-\frac{1}{2}, r}^n, s_{j+\frac{1}{2}, l}^n]$ regions where $s_{j+\frac{1}{2}, r}^n := s_{j+\frac{1}{2}} + c_{j+\frac{1}{2}}^n \Delta t^n$ and $s_{j+\frac{1}{2}, l}^n := s_{j+\frac{1}{2}} - c_{j+\frac{1}{2}}^n \Delta t^n$. This apportions a narrower Riemann fan of spatial width $\Delta s_{j+\frac{1}{2}} := s_{j+\frac{1}{2}, r}^n - s_{j+\frac{1}{2}, l}^n = 2c_{j+\frac{1}{2}}^n \Delta t^n$ around $s_{j+\frac{1}{2}}$ and Riemann-free interval of width $\Delta s_j := s_{j+\frac{1}{2}, l}^n - s_{j-\frac{1}{2}, r}^n = \Delta s - \Delta t^n (c_{j-\frac{1}{2}}^n + c_{j+\frac{1}{2}}^n)$ around s_j. Integration over non-uniform rectangles $[s_{j+\frac{1}{2}, l}^n, s_{j+\frac{1}{2}, r}^n] \times [t^n, t^{n+1}]$ and $[s_{j-\frac{1}{2}, r}^n, s_{j+\frac{1}{2}, l}^n] \times [t^n, t^{n+1}]$ gives intermediate cell-averages at t^{n+1},

$$\frac{1}{\Delta s_{j+\frac{1}{2}}} \int_{s_{j+\frac{1}{2}, l}^n}^{s_{j+\frac{1}{2}, r}^n} v(s, t^{n+1}) \, \mathrm{d}s = \frac{1}{\Delta s_{j+\frac{1}{2}}} \int_{s_{j+\frac{1}{2}, l}^n}^{s_{j+\frac{1}{2}, r}^n} \tilde{v}(s, t^n) \, \mathrm{d}s$$

$$- \frac{1}{\Delta s_{j+\frac{1}{2}}} \int_{t^n}^{t^{n+1}} F\left(v(s_{j+\frac{1}{2}, r}^n, t) \right) - F\left(v(s_{j+\frac{1}{2}, l}^n, t) \right) \, \mathrm{d}t,$$

and

$$\frac{1}{\Delta s_j} \int_{s_{j-\frac{1}{2}, r}^n}^{s_{j+\frac{1}{2}, l}^n} v(s, t^{n+1}) \, \mathrm{d}s = \frac{1}{\Delta s_j} \int_{s_{j-\frac{1}{2}, r}^n}^{s_{j+\frac{1}{2}, l}^n} \tilde{v}(s, t^n) \, \mathrm{d}s$$

$$- \frac{1}{\Delta s_j} \int_{t^n}^{t^{n+1}} F\left(v(s_{j+\frac{1}{2}, l}^n, t) \right) - F\left(v(s_{j-\frac{1}{2}, r}^n, t) \right) \, \mathrm{d}t,$$

where the flux integrals on the right hand side are approximated using the midpoint rule (Kurganov and Tadmor, 2000). The above equations are simplified to give respective cell-averages, $w_{j+\frac{1}{2}}^{n+1}$ and w_j^{n+1},

$$w_{j+\frac{1}{2}}^{n+1} = \frac{\bar{v}_j^n + \bar{v}_{j+1}^n}{2} + \frac{\Delta s - c_{j+\frac{1}{2}}^n \Delta t^n}{4} \left((v_s)_j^n - (v_s)_{j+1}^n \right) - \frac{1}{2c_{j+\frac{1}{2}}^n} \left[F\left(v_{j+\frac{1}{2}, r}^{n+\frac{1}{2}} \right) - F\left(v_{j+\frac{1}{2}, l}^{n+\frac{1}{2}} \right) \right], \tag{15}$$

$$w_j^{n+1} = \bar{v}_j^n + \frac{\Delta t^n}{2}\left(c_{j-\frac{1}{2}}^n - c_{j+\frac{1}{2}}^n\right)(v_s)_j^n - \frac{\lambda^n}{1 - \lambda^n\left(c_{j-\frac{1}{2}}^n + c_{j+\frac{1}{2}}^n\right)}\left[F\left(v_{j+\frac{1}{2},l}^{n+\frac{1}{2}}\right) - F\left(v_{j-\frac{1}{2},r}^{n+\frac{1}{2}}\right)\right], \quad (16)$$

with mesh ratio $\lambda^n = \frac{\Delta t^n}{\Delta s}$ and mid-values $v_{j\pm\frac{1}{2},r}^{n+\frac{1}{2}}$ and $v_{j\pm\frac{1}{2},l}^{n+\frac{1}{2}}$ obtained using the Taylor series expansion,

$$v_{j+\frac{1}{2},l}^{n+\frac{1}{2}} := v_{j+\frac{1}{2},l}^n - \frac{\Delta t^n}{2}F\left(v_{j+\frac{1}{2},l}^n\right)_s \quad \text{and} \quad v_{j+\frac{1}{2},r}^{n+\frac{1}{2}} := v_{j+\frac{1}{2},r}^n - \frac{\Delta t^n}{2}F\left(v_{j+\frac{1}{2},r}^n\right)_s, \quad (17)$$

where

$$v_{j+\frac{1}{2},l}^n := v_j^n + \Delta s(v_s)_j^n\left(\frac{1}{2} - \lambda^n c_{j+\frac{1}{2}}^n\right) \quad \text{and} \quad v_{j+\frac{1}{2},r}^n := v_{j+1}^n - \Delta s(v_s)_{j+1}^n\left(\frac{1}{2} - \lambda^n c_{j+\frac{1}{2}}^n\right).$$

• **Projection Step:** Based on (15) and (16), a linear piecewise interpolant is reconstructed, which gives

$$\tilde{w}(s,\,t^{n+1}) := \sum_j\left\{\left[w_{j+\frac{1}{2}}^{n+1} + (v_s)_{j+\frac{1}{2}}^{n+1}(s - s_{j+\frac{1}{2}})\right]\chi_{[s_{j+\frac{1}{2},l}^n,\,s_{j+\frac{1}{2},r}^n]} + w_j^{n+1}\chi_{[s_{j-\frac{1}{2},r}^n,\,s_{j+\frac{1}{2},l}^n]}\right\}, \quad (18)$$

where

$$(v_s)_{j+\frac{1}{2}}^{n+1} := \frac{2}{\Delta s}\text{MM}\left(\frac{w_{j+1}^{n+1} - w_{j+\frac{1}{2}}^{n+1}}{1 + \lambda^n\left(c_{j+\frac{1}{2}}^n - c_{j+\frac{3}{2}}^n\right)}, \frac{w_{j+\frac{1}{2}}^{n+1} - w_j^{n+1}}{1 + \lambda^n\left(c_{j+\frac{1}{2}}^n - c_{j-\frac{1}{2}}^n\right)}\right).$$

Averages of (18) are projected onto the original grid $[s_{j-\frac{1}{2}},\,s_{j+\frac{1}{2}}]$, giving the fully discrete KT scheme

$$\begin{aligned}
v_j^{n+1} &= \frac{1}{\Delta s}\int_{s_{j-\frac{1}{2}}}^{s_{j+\frac{1}{2}}}\tilde{w}(s,\,t^{n+1})\,\mathrm{d}s \\
&= \lambda^n c_{j-\frac{1}{2}}^n w_{j-\frac{1}{2}}^{n+1} + \left[1 - \lambda^n\left(c_{j-\frac{1}{2}}^n - c_{j+\frac{1}{2}}^n\right)\right]w_j^{n+1} \\
&\quad + \lambda^n c_{j+\frac{1}{2}}^n w_{j+\frac{1}{2}}^{n+1} + \frac{\Delta s}{2}\left[\left(\lambda^n c_{j-\frac{1}{2}}^n\right)^2(v_s)_{j-\frac{1}{2}}^{n+1} - \left(\lambda^n c_{j+\frac{1}{2}}^n\right)^2(v_s)_{j+\frac{1}{2}}^{n+1}\right].
\end{aligned} \quad (19)$$

Using (19) with (15)-(16) and letting $\Delta t^n \downarrow 0$ in $\frac{v_j^{n+1} - v_j^n}{\Delta t^n}$ gives the semi-discrete KT scheme for PDE (10),

$$\frac{\mathrm{d}}{\mathrm{d}t}v_j(t) = -\frac{H_{j+\frac{1}{2}}(t) - H_{j-\frac{1}{2}}(t)}{\Delta s}, \quad (20)$$

$$H_{j+\frac{1}{2}} := \frac{1}{2}\left[F\left(v_{j+\frac{1}{2}}^+\right) + F\left(v_{j+\frac{1}{2}}^-\right)\right] - \frac{c_{j+\frac{1}{2}}}{2}\left(v_{j+\frac{1}{2}}^+ - v_{j+\frac{1}{2}}^-\right),$$

where H represents the numerical flux and midvalues (17) of (19) approach (14) as $\Delta t^n \to 0$. Kurganov and Tadmor (2000) extended (20) to the convection-diffusion-reaction PDE in the conservative form,

$$\frac{\partial v}{\partial t} + \frac{\partial}{\partial s}F(v) = \frac{\partial}{\partial s}Q(v,\,v_s) + S(v), \quad (21)$$

with diffusion flux, Q and possibly existing source term, S. The semi-discrete KT scheme for (21) gives

$$\frac{\mathrm{d}}{\mathrm{d}t}v_j(t) = -\frac{H_{j+\frac{1}{2}}(t) - H_{j-\frac{1}{2}}(t)}{\Delta s} + \frac{P_{j+\frac{1}{2}}(t) - P_{j-\frac{1}{2}}(t)}{\Delta s} + S\left(v_j(t)\right), \quad (22)$$

where P denotes an approximation of Q and obtained using basic forward and backward differencing,

$$P_{j+\frac{1}{2}} := \frac{1}{2}\left[Q\left(v_j,\,\frac{v_{j+1} - v_j}{\Delta s}\right) + Q\left(v_{j+1},\,\frac{v_{j+1} - v_j}{\Delta s}\right)\right].$$

3.1 Two-Dimensional Extension

Kurganov and Tadmor (2000) extended (22) to the two-dimensional convection-diffusion-reaction PDE,

$$\frac{\partial v}{\partial t} + \frac{\partial}{\partial s} F^s(v) + \frac{\partial}{\partial a} F^a(v) = \frac{\partial}{\partial s} Q^s(v, v_s, v_a) + \frac{\partial}{\partial a} Q^a(v, v_s, v_a) + S(v). \tag{23}$$

in spatial variables s and a. For mesh $(s_j, a_k) = (j\Delta s, k\Delta a)$, the semi-discrete KT for (23) is given by

$$\frac{\mathrm{d}}{\mathrm{d}t} v_{j,k}(t) = -\frac{H^s_{j+\frac{1}{2}, k}(t) - H^s_{j-\frac{1}{2}, k}(t)}{\Delta s} - \frac{H^a_{j, k+\frac{1}{2}}(t) - H^a_{j, k-\frac{1}{2}}(t)}{\Delta a} \\ + \frac{P^s_{j+\frac{1}{2}, k}(t) - P^s_{j-\frac{1}{2}, k}(t)}{\Delta s} + \frac{P^a_{j, k+\frac{1}{2}}(t) - P^a_{j, k-\frac{1}{2}}(t)}{\Delta a} + S\left(v_{j,k}(t)\right), \tag{24}$$

where the s and a numerical fluxes $H^s_{j+\frac{1}{2}, k}$, $H^a_{j, k+\frac{1}{2}}$ and diffusive fluxes $P^s_{j+\frac{1}{2}, k}$, $P^a_{j, k+\frac{1}{2}}$ are given by

$$H^s_{j+\frac{1}{2}, k} := \frac{1}{2}\left[F^s\left(v^+_{j+\frac{1}{2}, k}\right) + F^s\left(v^-_{j+\frac{1}{2}, k}\right)\right] - \frac{c^s_{j+\frac{1}{2}, k}}{2}\left(v^+_{j+\frac{1}{2}, k} - v^-_{j+\frac{1}{2}, k}\right),$$

$$H^a_{j, k+\frac{1}{2}} := \frac{1}{2}\left[F^a\left(v^+_{j, k+\frac{1}{2}}\right) + F^a\left(v^-_{j, k+\frac{1}{2}}\right)\right] - \frac{c^a_{j, k+\frac{1}{2}}}{2}\left(v^+_{j, k+\frac{1}{2}} - v^-_{j, k+\frac{1}{2}}\right),$$

and

$$P^s_{j+\frac{1}{2}, k} := \frac{1}{2}\left[Q^s\left(v_{j,k}, \frac{v_{j+1,k} - v_{j,k}}{\Delta s}, (v_a)_{j,k}\right) + Q^s\left(v_{j+1,k}, \frac{v_{j+1,k} - v_{j,k}}{\Delta s}, (v_a)_{j+1,k}\right)\right],$$

$$P^a_{j, k+\frac{1}{2}} := \frac{1}{2}\left[Q^a\left(v_{j,k}, (v_s)_{j,k}, \frac{v_{j,k+1} - v_{j,k}}{\Delta a}\right) + Q^a\left(v_{j,k+1}, (v_s)_{j,k+1}, \frac{v_{j,k+1} - v_{j,k}}{\Delta a}\right)\right].$$

In the above equations, intermediate values $v^\pm_{j+\frac{1}{2}, k}$, $v^\pm_{j, k+\frac{1}{2}}$ and local speeds $c^s_{j+\frac{1}{2}, k}$, $c^a_{j, k+\frac{1}{2}}$ are given by

$$v^\pm_{j+\frac{1}{2}, k} := v_{j+1, k} \mp \frac{\Delta s}{2}(v_s)_{j+\frac{1}{2}\pm\frac{1}{2}, k} \;\; \text{and} \;\; v^\pm_{j, k+\frac{1}{2}} := v_{j, k+1} \mp \frac{\Delta a}{2}(v_a)_{j, k+\frac{1}{2}\pm\frac{1}{2}},$$

$$c^s_{j+\frac{1}{2}, k} := \max_\pm\left(\left|\frac{\partial F^s}{\partial v}\left(v^\pm_{j+\frac{1}{2}, k}\right)\right|\right) \;\; \text{and} \;\; c^a_{j, k+\frac{1}{2}} := \max_\pm\left(\left|\frac{\partial F^a}{\partial v}\left(v^\pm_{j, k+\frac{1}{2}}\right)\right|\right).$$

3.2 Conservative Form of Black-Scholes PDEs

We solve (1) as a forward-in-time PDE with $t^* = T - t$ and we denote the reversed time t^* again with t, giving

$$\frac{\partial v}{\partial t} - \frac{1}{2}\sigma^2 s^2 \frac{\partial^2 v}{\partial s^2} - (r - \delta)s \frac{\partial v}{\partial s} + rv = 0, \tag{25}$$

which transforms terminal payoff $v(s, T)$ into initial condition $v(s, 0)$. In conformity to (22), using

$$\frac{\partial}{\partial s}(sv) = s\frac{\partial v}{\partial s} + v \;\; \text{and} \;\; \frac{\partial}{\partial s}\left(s^2\frac{\partial v}{\partial s}\right) = s^2\frac{\partial^2 v}{\partial s^2} + 2s\frac{\partial v}{\partial s},$$

Ramírez-Espinoza and Ehrhardt (2013) rewrote (25) in the form (21),

$$\frac{\partial v}{\partial t} + \frac{\partial}{\partial s}\left((\sigma^2 - r + \delta)sv\right) = \frac{\partial}{\partial s}\left(\frac{1}{2}\sigma^2 s^2\frac{\partial v}{\partial s}\right) + (\sigma^2 - 2r + \delta)v, \tag{26}$$

with convection flux $F(s, v) := (\sigma^2 - r + \delta)sv$, diffusion flux $Q(s, v) := \frac{1}{2}\sigma^2 s^2\frac{\partial v}{\partial s}$ and source term $S(v) := (\sigma^2 - 2r + \delta)v$. In particular, PDE (26) prices European options for initial conditions,

$$v(s, 0) = \max(s - K, 0) \;\; \text{for call} \;\; \text{and} \;\; v(s, 0) = \max(K - s, 0) \;\; \text{for put}, \tag{27}$$

obtained from (2) and for corresponding boundary conditions, as described in (3), such that, for

$$
\text{call} \quad
\begin{cases}
v(s_{\min}, t) & = 0, \\
v(s_{\max}, t) & = s_{\max} \exp(-\delta t) - K \exp(-rt),
\end{cases}
$$

$$
\text{put} \quad
\begin{cases}
v(s_{\min}, t) & = K \exp(-rt) - s_{\min} \exp(-\delta t), \\
v(s_{\max}, t) & = 0.
\end{cases}
\tag{28}
$$

Similarly, Ramírez-Espinoza and Ehrhardt (2013) rewrote (7) as a forward-in-time PDE in the form (23),

$$
\frac{\partial v}{\partial t} + \frac{\partial}{\partial s}(\sigma^2 - r)sv - \frac{\partial}{\partial a}\left(\frac{1}{T-t}(s-a)v\right) = \frac{\partial}{\partial s}\left(\frac{1}{2}\sigma^2 s^2 \frac{\partial v}{\partial s}\right) + \left(\sigma^2 - 2r + \frac{1}{T-t}\right)v,
\tag{29}
$$

with convective fluxes $F^s(s, v) := (\sigma^2 - r)sv$ and $F^a(s, a, v) := -\frac{1}{T-t}(s-a)v$ respectively in $s-$ and $a-$direction, diffusive flux $Q^s(s, v, v_s) := \frac{1}{2}\sigma^2 s^2 \frac{\partial v}{\partial s}$ which exists only in $s-$direction and source term $S(v) := \left(\sigma^2 - 2r + \frac{1}{T-t}\right)v$. PDE (29) solves Asian options with payoff functions (8) converted into initial conditions $v(s, a, 0)$, such that, for

$$
\text{call} \quad
\begin{cases}
\max(a - K, 0) & \text{fixed strike}, \\
\max(s - a, 0) & \text{floating strike},
\end{cases}
\qquad
\text{put} \quad
\begin{cases}
\max(K - a, 0) & \text{fixed strike}, \\
\max(a - s, 0) & \text{floating strike}.
\end{cases}
\tag{30}
$$

For Asian put options, Ramírez-Espinoza and Ehrhardt (2013) bypassed the intricate discretisation of (9), giving for

$$
\text{fixed strike} \quad
\begin{cases}
v(s_{\min}, a, t) & = \max\left(0, K - \frac{1}{T}(T-t)a\right)\exp(-rt), \\
v(s_{\max}, a, t) & = \max\left(0, K - \frac{1}{T}[s_{\max}t + a(T-t)]\right),
\end{cases}
\tag{31}
$$

$$
\text{floating strike} \quad
\begin{cases}
v(s_{\min}, a, t) & = \max\left(0, -s_{\min} + \frac{1}{T}(T-t)a\right)\exp(-rt), \\
v(s_{\max}, a, t) & = \max\left(0, -s_{\max} + \frac{1}{T}[s_{\max}t + a(T-t)]\right).
\end{cases}
\tag{32}
$$

4 Effective implementations

We describe some implementations to effectively solve option pricing PDEs using the conservative KT scheme.

4.1 Time Solvers

The overall high accuracy of spatial reconstruction is retained by using high-order stable time discretisations (Kurganov and Tadmor, 2000). In line, Ramírez-Espinoza and Ehrhardt (2013) used the MATLAB in-built ode15s solver (Shampine and Reichelt, 1997), which is based on an implicit multi-step Runge-Kutta (RK) method. It achieves fast and excellent numerical solutions for one-dimensional problems but suffers from high computational effort in two-dimensional cases (Ramírez-Espinoza, 2011).

In amendment, we propose efficient use of the MATLAB ODE suite. As indicated in Shampine and Reichelt (1997), we use the ode45 function, which is based on an one-step explicit RK formula, as the 'first-try' time solver. In case ode45 acts inefficient by slowing down computation mostly due to the presence of stiff systems, we automatically shift to ode15s. For instance, Zhao et al. (2007) used ode15s for pricing American options in the presence of a stiff ODE due to very small time step requirement.

Also, amongst several time methods discussed in Gottlieb et al. (2001), we propose the second-order two-steps explicit RK time differencing. Denoting $L(v_j) := \frac{\mathrm{d}}{\mathrm{d}t}v_j(t)$ as an approximation to ODE (22), the one-parameter explicit two-stages RK method as described in Gottlieb et al. (2001), gives

$$
v^{(1)} = v^n + \Delta t^n L(v^n),
$$

$$
v^{n+1} = \frac{1}{2}v^n + \frac{1}{2}\left(v^{(1)} + \Delta t^n L(v^{(1)})\right).
$$

4.2 Slope Limiters

The non-oscillatory behaviour and thus high-resolution property of central schemes rely on the appropriate choice of slope limiters. As such, Ramírez-Espinoza and Ehrhardt (2013) obtained non-oscillatory numerical solutions and Greeks despite non-smooth data by using (12). As compared to the most dissipative $\theta = 1$ and least dissipative $\theta = 2$, $\theta = 1.5$ is optimal (Kurganov and Tadmor, 2000; Ramírez-Espinoza and Ehrhardt, 2013). However, in two-dimensional cases, Ramírez-Espinoza (2011) implemented (12) in C, compiled with the MEX utility of the MATLAB suite to avoid excessive computation time requisite to element-wise operations. As reported in Ramírez-Espinoza (2011), this changed the execution time from ~ 10 to ~ 4 minutes for fixed strike and from ~ 40 to $\sim 6 - 8$ minutes for floating strike; results were recorded using a CPU with 8 GB of RAM memory. We propose to bypass the heavy time consuming loops of (12) using the fully vectorised approach (Peer et al., 2008),

$$\text{MM}(z_1, z_2, z_3) = \frac{1}{4} \left[\text{sign}(z_1) + \text{sign}(z_2) + \text{sign}(z_3) + \text{sign}(z_1 z_2 z_3) \right] \times \min(|z_1|, |z_2|, |z_3|). \qquad (33)$$

Also, we propose the uniform non-oscillatory (UNO) limiter, developed by Harten and Osher (1987) and adapted by Nessyahu and Tadmor (1990) using the central differencing $\Delta^2 v_j \equiv v_{j+1} - 2v_j + v_{j-1}$, to give

$$(v_s)_j := \text{MM} \left(\Delta v_{j-\frac{1}{2}} + \frac{1}{2} \text{MM}(\Delta^2 v_{j-1}, \Delta^2 v_j), \Delta v_{j+\frac{1}{2}} - \frac{1}{2} \text{MM}(\Delta^2 v_j, \Delta^2 v_{j+1}) \right). \qquad (34)$$

It offers higher resolution even at critical grid values as compared to the original $\theta = 1$ limiter of (12).

4.3 Code Structure

Below we summarise the fully vectorised algorithm of the conservative KT scheme (22) applied to (26).

(1) Define parameters σ, r, δ, K, T, $s_{\min}$ and $s_{\max}$, flux handles F, Q, S of (26), boundary functions $BC_1(t)$ and $BC_2(t)$ for $t \in [0, T]$ and initial condition $v(s, 0)$.

(2) Define uniform spatial discretisation of size $N + 1$ with $\Delta s = (s_{\max} - s_{\min})/N$.

(3) Until $t^{n+1} := t^n + \Delta t^n > T$, compute

   (a) spatial derivatives $(v_s)_j$ of (11) using the MM (33) or UNO (34) limiter and use extrapolation technique to compute boundary values $(v_s)_1$ and $(v_s)_{N+1}$,

   (b) local speeds $c^n_{j\pm\frac{1}{2}}$ of (13) and intermediate values $v^{\pm}_{j\pm\frac{1}{2}}$ of (14),

   (c) functions H, P, S and $\frac{\mathrm{d}}{\mathrm{d}t} v_j(t)$ of the semi-discrete KT formula (22),

   (d) solution v^{n+1} using appropriate time solver from Section 4.1,

   (e) boundary values $BC_1(t)$ and $BC_2(t)$ at t^{n+1}.

The above algorithm is effortlessly extended to two-dimensions to solve (23) using formula (24). We maintain the fully vectorised setup with a spatial grid of size $(N + 1) \times (N + 1)$.

4.4 American Options

We apply the conservative KT method (22) to price American put options under (26) with or without dividend, subject to initial condition (27), boundary conditions as described in (5), giving for

$$\text{call} \quad \begin{cases} v(s_{\min}, t) &= 0, \\ v(s_{\max}, t) &= s_{\max} - K, \end{cases} \qquad \text{put} \quad \begin{cases} v(s_{\min}, t) &= K - s_{\min}, \\ v(s_{\max}, t) &= 0, \end{cases} \qquad (35)$$

and early constraint (6). To our knowledge, this is the first time that American options are priced by extending (22) to include (6). For fully discrete schemes, (6) is imposed on intermediate values $v_j(t)$ before each time evolution,

$$v_j(t) = \max \left(v_j(t), v_j^0 \right). \qquad (36)$$

The semi-discrete KT method treats spatial reconstruction and time evolution separately with no change in time within the spatial reconstruction. Therefore, in conformity to KT, we apply (36) to (22), giving

$$\frac{\mathrm{d}}{\mathrm{d}t} v_j(t) = \max\left(\frac{\mathrm{d}}{\mathrm{d}t} v_j(t), 0\right),$$

which is easily incorporated in the algorithm described in Section 4.3.

4.5 Barrier Options

Also, we price exotic barrier options. The payoff depends on whether before expiry the underlying asset's price reaches the predefined barrier level, set above (up) or below (down) the asset price. Barrier options come into existence (in) when asset price exceeds an upper barrier (up-and-in) or falls below a lower barrier (down-and-in). Barrier options which are in existence, are extinguished (out) when asset price exceeds an upper barrier (up-and-out) or falls below a lower barrier (down-and-out).

We extend the algorithm in Section 4.3 to solve call up-and-out barrier options for initial condition

$$v(s, 0) = \begin{cases} \max(s - K, 0), & 0 \leq s < B, \\ 0, & s \geq B, \end{cases}$$

and boundary conditions $v(s, t) = 0$ as $s \to 0$ and $v(s, t) = 0$ as $s \to \infty$, with upper barrier B. To the author's knowledge, this is the first time that KT is applied to solve call up-and-out barrier options by enforcing the barrier level condition to output of (22), at each time step,

$$\frac{\mathrm{d}}{\mathrm{d}t} v_j(t) = 0, \quad \text{for} \quad s_j \geq B.$$

4.6 Second-Order Extensions

Also, we compare results of KT to its second-order conservative extensions by Kurganov et al. (2001) and Kurganov and Lin (2007), denoted by KNP and KL respectively.

The main idea of KNP retains the reconstruction and projection of KT with more precise use of one-sided local speeds. The local speed (13) of KT is replaced by left and right one-sided local speeds,

$$\begin{aligned}
c_{j+\frac{1}{2}}^+ &:= \max\left(\frac{\partial F}{\partial v}\left(v_{j+\frac{1}{2}}^-\right), \frac{\partial F}{\partial v}\left(v_{j+\frac{1}{2}}^+\right), 0\right), \\
c_{j+\frac{1}{2}}^- &:= \min\left(\frac{\partial F}{\partial v}\left(v_{j+\frac{1}{2}}^-\right), \frac{\partial F}{\partial v}\left(v_{j+\frac{1}{2}}^+\right), 0\right),
\end{aligned} \tag{37}$$

where $v_{j+\frac{1}{2}}^-$ and $v_{j+\frac{1}{2}}^+$ are given in (14). For evolution step, the new intermediate cell-averages $w_{j+\frac{1}{2}}^{n+1}$ and w_j^{n+1} are computed by integrating over the volumes $[s_{j+\frac{1}{2},l}^n, s_{j+\frac{1}{2},r}^n] \times [t^n, t^{n+1}]$ and $[s_{j-\frac{1}{2},r}^n, s_{j+\frac{1}{2},l}^n] \times [t^n, t^{n+1}]$ respectively, where $s_{j+\frac{1}{2},r}^n := s_{j+\frac{1}{2}} + c_{j+\frac{1}{2}}^+ \Delta t$ and $s_{j+\frac{1}{2},l}^n := s_{j+\frac{1}{2}} + c_{j+\frac{1}{2}}^- \Delta t$. At the final step, the projection technique is similar to KT. The new convection flux of the semi-discrete KNP scheme reads

$$H_{j+\frac{1}{2}} := \frac{c_{j+\frac{1}{2}}^+ F\left(v_{j+\frac{1}{2}}^-\right) - c_{j+\frac{1}{2}}^- F\left(v_{j+\frac{1}{2}}^+\right)}{c_{j+\frac{1}{2}}^+ - c_{j+\frac{1}{2}}^-} + \frac{c_{j+\frac{1}{2}}^+ c_{j+\frac{1}{2}}^-}{c_{j+\frac{1}{2}}^+ - c_{j+\frac{1}{2}}^-}\left(v_{j+\frac{1}{2}}^+ - v_{j+\frac{1}{2}}^-\right).$$

The less dissipative KL scheme retains the reconstruction and evolution steps of KNP and is based on more accurate projection. Based on new cell-averages $\bar{w}_{j+\frac{1}{2}}^{n+1}$ and $\bar{w}_j^{n+1}$, the linear reconstruction (Kurganov et al., 2001; Kurganov and Lin, 2007) reads

$$\tilde{w}(s, t^{n+1}) := \sum_j \left\{\left[\bar{w}_{j+\frac{1}{2}}^{n+1} + (v_s)_{j+\frac{1}{2}}^{n+1}\left(s - \frac{s_{j+\frac{1}{2},l}^n + s_{j+\frac{1}{2},r}^n}{2}\right)\right] \chi_{[s_{j+\frac{1}{2},l}^n, s_{j+\frac{1}{2},r}^n]} + \bar{w}_j^{n+1} \chi_{[s_{j-\frac{1}{2},r}^n, s_{j+\frac{1}{2},l}^n]}\right\},$$

where

$$(v_s)_{j+\frac{1}{2}}^{n+1} = \frac{2}{\Delta t^n} \mathrm{MM} \left(\frac{\bar{w}_{j+\frac{1}{2}}^{n+1} - v_{j+\frac{1}{2},l}^{n+1}}{c_{j+\frac{1}{2}}^+ - c_{j+\frac{1}{2}}^-}, \; \frac{v_{j+\frac{1}{2},r}^{n+1} - \bar{w}_{j+\frac{1}{2}}^{n+1}}{c_{j+\frac{1}{2}}^+ - c_{j+\frac{1}{2}}^-} \right),$$

represents a less dissipative slope, with $c_{j+\frac{1}{2}}^\pm$ of (37) and $v_{j+\frac{1}{2},l}^{n+1}$, $v_{j+\frac{1}{2},r}^{n+1}$ of (17). Following simplification, the convection flux of KL is given by

$$H_{j+\frac{1}{2}} := \frac{c_{j+\frac{1}{2}}^+ F\left(v_{j+\frac{1}{2}}^-\right) - c_{j+\frac{1}{2}}^- F\left(v_{j+\frac{1}{2}}^+\right)}{c_{j+\frac{1}{2}}^+ - c_{j+\frac{1}{2}}^-} + c_{j+\frac{1}{2}}^+ c_{j+\frac{1}{2}}^- \left(\frac{v_{j+\frac{1}{2}}^+ - v_{j+\frac{1}{2}}^-}{c_{j+\frac{1}{2}}^+ - c_{j+\frac{1}{2}}^-} - q_{j+\frac{1}{2}} \right).$$

In the above, $q_{j+\frac{1}{2}}$ denotes the correction term, which accounts for reduced dissipation and is given by

$$q_{j+\frac{1}{2}} = \mathrm{MM} \left(\frac{v_{j+\frac{1}{2}}^+ - w_{j+\frac{1}{2}}^{\mathrm{int}}}{c_{j+\frac{1}{2}}^+ - c_{j+\frac{1}{2}}^-}, \; \frac{w_{j+\frac{1}{2}}^{\mathrm{int}} - v_{j+\frac{1}{2}}^-}{c_{j+\frac{1}{2}}^+ - c_{j+\frac{1}{2}}^-} \right),$$

where

$$w_{j+\frac{1}{2}}^{\mathrm{int}} = \frac{c_{j+\frac{1}{2}}^+ v_{j+\frac{1}{2}}^+ - c_{j+\frac{1}{2}}^- v_{j+\frac{1}{2}}^- - \left[F\left(v_{j+\frac{1}{2}}^+\right) - F\left(v_{j+\frac{1}{2}}^-\right) \right]}{c_{j+\frac{1}{2}}^+ - c_{j+\frac{1}{2}}^-},$$

represent the intermediate values.

The conservative KNP and KL "Black-Box" methods are each adapted to option pricing PDEs by updating the algorithm in Section 4.3 to include any additional term and improved convection flux.

5 Numerical Experiments

In this paper, for all experiments, we have used a computer with 8 GB RAM and a 2.50 GHz Intel(R) Core(TM) i5-3210M processor. The error norms and root mean square (RMS) error are given by

$$L_1 \text{ error} = \frac{1}{N} \sum_j \left| v(s_j, \, t^n) - v_j^n \right|,$$

$$L_\infty \text{ error} = \max_j \left| v(s_j, \, t^n) - v_j^n \right|,$$

$$\text{RMS error} = \sqrt{\frac{1}{N_1} \sum_j \left(v(s_j, \, t^n) - v_j^n \right)^2},$$

where $N_1 \leq N$ is the number of asset prices s considered.

5.1 European Options

Problem 5.1 We solve the convection-dominated European problem arising from high Péclet ratio. According to Zvan et al. (1998), high Péclet condition tends to introduce spurious oscillations in numerical solutions. Therefore, though financially unrealistic, this test case is used to assess the behaviour of KT. For a European call, we extract from Ramírez-Espinoza and Ehrhardt (2013) the parameters $\sigma = 0.02$, $r = 0.46$, $\delta = 0.00$, $T = 1.00$, $K = 70$, $s \in [0, \, 100]$ and Péclet $\propto \frac{r}{\sigma^2} = 1150$. This requires solving (26) subject to conditions (27) and (28), using the algorithm in Section 4.3.

For Problem 5.1, we use the MM limiter (33) with $\theta = 1$, 1.5 and 2 and ode45. Table 5.1 shows corresponding L_1 and L_∞ errors and convergence rates. KT converges to second-order accuracy under both norms. According to Serna and Marquina (2004), the expected maximum order of accuracy is not achieved due to the non-linearity of limiters. In line with Kurganov and Tadmor (2000) and Ramírez-Espinoza and Ehrhardt (2013), we note that $\theta = 1.5$ offers the least L_1 and L_∞ errors as compared to

Table 5.1: Accuracy for Problem 5.1.

	N	L_1 Norm	L_1 Order	L_∞ Norm	L_∞ Order
$\theta = 1.0$	100	1.4282e-02	-	2.6475e-01	-
	200	4.5606e-03	1.6469	1.2121e-01	1.1271
	400	1.2421e-03	1.8765	4.1940e-02	1.5311
	800	3.1205e-04	1.9929	1.1015e-02	1.9288
	1600	7.8126e-05	1.9979	2.6905e-03	2.0336
$\theta = 1.5$	100	8.8154e-04	-	2.1355e-02	-
	200	8.2756e-04	0.0912	4.1158e-02	-0.9466
	400	4.9558e-04	0.7397	2.4075e-02	0.7737
	800	1.5103e-04	1.7143	5.4452e-03	2.1445
	1600	3.8703e-05	1.9643	1.3710e-03	1.9897
$\theta = 2.0$	100	1.0899e-03	-	4.3721e-02	-
	200	1.0383e-03	0.0700	5.3321e-02	-0.2864
	400	5.1969e-04	0.9985	2.6277e-02	1.0209
	800	1.5240e-04	1.7698	5.4868e-03	2.2598
	1600	3.8791e-05	1.9741	1.3743e-03	1.9972
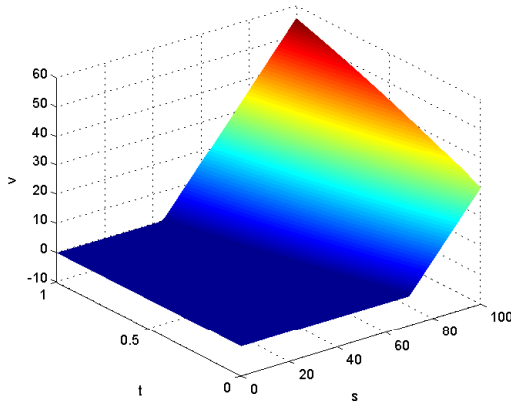
(a) Surface for $0 \le t \le T$
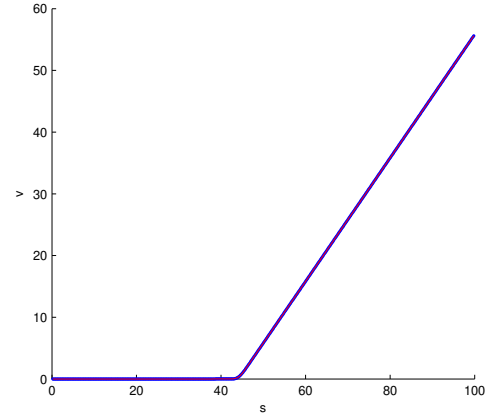
(b) Option price, v
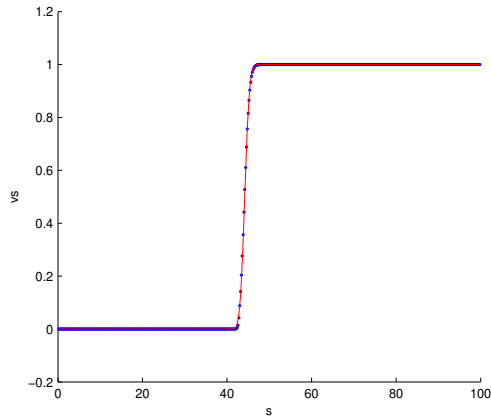
(c) Delta, v_s
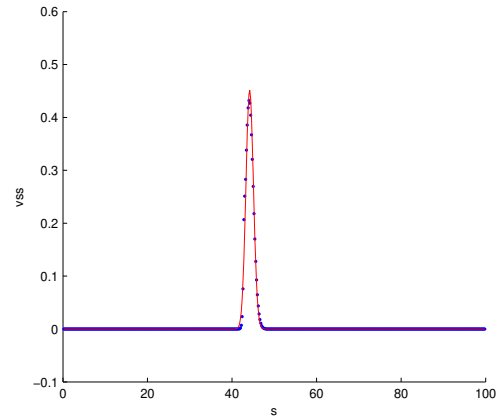
(d) Gamma, v_{ss}

Figure 5.1: Solutions for Problem 5.1.

$\theta = 1$ and 2. Fig 5.1 displays the surface for $0 \le t \le T$, option price and Greeks for Problem 5.1

Table 5.2: Accuracy for Problems 5.2 and 5.3.

	Standard Problem			
N	L_1 Norm	L_1 Order	L_∞ Norm	L_∞ Order
10	1.7615e-01	-	1.5181e-00	-
20	4.4662e-02	1.9797	3.5080e-01	2.1136
40	1.1350e-02	1.9763	7.9784e-02	2.1365
80	2.8270e-03	2.0054	1.9974e-02	1.9980
160	7.0882e-04	1.9958	4.9923e-03	2.0004
320	1.7757e-04	1.9970	1.2498e-03	1.9980
640	4.4486e-05	1.9970	3.1281e-04	1.9984
	Challenging Problem			
N	L_1 Norm	L_1 Order	L_∞ Norm	L_∞ Order
10	1.0291e-01	-	9.9149e-01	-
20	5.0449e-02	1.0285	9.3223e-01	0.0889
40	2.2148e-02	1.1876	7.2631e-01	0.3601
80	6.5990e-03	1.7468	3.2583e-01	1.1564
160	1.5945e-03	2.0492	1.3339e-01	1.2885
320	2.8251e-04	2.4967	2.8039e-02	2.2501
640	4.0628e-05	2.7977	1.0827e-02	1.3728

using MM limiter (33) with $\theta = 1.5$ and $N = 500$. We observe that in line with Ramírez-Espinoza and Ehrhardt (2013), KT offers excellent, non-oscillatory and high-resolution approximations despite the convectively dominated setup, non-smoothness in initial condition and discontinuities in Greeks.

We repeat the experiment for Problem 5.1 with RK2 described in Section 4.1. We observe that ode45 offers smaller error and slightly better convergence than RK2. Also, we solve Problem 5.1 using UNO limiter (34), which output errors and convergence rates almost similar to MM limiter (33). Next, we solve Problem 5.1 using KNP and KL. We observe that KNP and KL offer almost identical error norms and convergence rates as KT with insignificant difference in computation time. Therefore, for further experiments, we use KT and MM limiter (33) with $\theta = 1.5$.

We confirm the aptitude of KT by solving the standard and challenging European call benchmark options from von Sydow et al. (2015). The respective sets of parameters are given below:

Problem 5.2 Standard parameters: $\sigma = 0.15$, $r = 0.03$, $\delta = 0.00$, $T = 1.00$, $K = 100$, and $s \in [0, 200]$.

Problem 5.3 Challenging parameters: $\sigma = 0.01$, $r = 0.10$, $\delta = 0.00$, $T = 0.25$, $K = 100$ and $s \in [0, 200]$.

Table 5.2 records the L_1 and L_∞ errors and convergence rates for Problem 5.2 and 5.3 using ode45. For both problems, KT achieves quadratic convergence under L_1 norm. However, under L_∞ norm, second-order accuracy is achieved only for the standard problem and a drop in accuracy occurs for the challenging case. As observed in Peer et al. (2008), a drop in L_∞ convergence may occur in the presence of discontinuity, which is the case for the challenging problem.

5.2 American Options

Problem 5.4 We price American put options for different sets of parameters from Tangman et al. (2008), with short maturity $T = 0.50$, $s \in [0, 200]$ and $N = 400$ using ode45. Numerical solutions for short maturity options tend to be non-smooth such that error introduced due to kink at strike price is not easily damped. We extend the KT algorithm in Section 4.3 to incorporate the early constraint as described in Section 4.4.

For Problem 5.4, we use reference values from Tangman et al. (2008) and Leisen and Reimer (1996). For different sets of parameters, Table 5.3 compares at different asset prices $s = 80, 90, 100, 110, 120,$

Table 5.3: Option value and Greeks for Problem 5.4.

	$r = 0.05$ $\sigma = 0.20$ $\delta = 0.00$		$r = 0.07$ $\sigma = 0.40$ $\delta = 0.03$		$r = 0.10$ $\sigma = 0.30$ $\delta = 0.05$	
	Option Value					
s	KT	Reference	KT	Reference	KT	Reference
80	20.0000	20.0000	21.8706	21.8709	20.2575	20.2578
90	10.6653	10.6661	15.2292	15.2297	12.5974	12.5980
100	4.6547	4.6557	10.2381	10.2387	7.2763	7.2770
110	1.6674	1.6680	6.6774	6.6680	3.9224	3.9230
120	0.4974	0.4976	4.2470	4.2476	1.9903	1.9907

	$r = 0.07$ $\sigma = 0.40$ $\delta = 0.03$		$r = 0.07$ $\sigma = 0.40$ $\delta = 0.03$	
	Delta Value		Gamma Value	
s	KT	Reference	KT	Reference
80	-0.7501	-0.7501	0.0172	0.0172
90	-0.5791	-0.5791	0.0166	0.0166
100	-0.4230	-0.4229	0.0144	0.0144
110	-0.2943	-0.2943	0.0113	0.0113
120	-0.1968	-0.1968	0.0083	0.0083

Table 5.4: RMS errors for Problem 5.4.

Scheme	$r = 0.05$ $\sigma = 0.20$ $\delta = 0.00$	$r = 0.07$ $\sigma = 0.40$ $\delta = 0.03$	$r = 0.10$ $\sigma = 0.30$ $\delta = 0.05$
Brennan Schwartz 1	3.5491e-03	8.5740e-03	5.9444e-03
Brennan Schwartz 2	6.9714e-04	5.8822e-04	6.1156e-04
CN PSOR	8.3307e-04	8.8204e-04	7.9750e-04
Borici Luthi	6.0498e-04	4.7749e-04	5.1769e-04
Penalty 1	9.3915e-04	1.1145e-03	9.8489e-04
Penalty 2	7.4993e-03	2.7882e-03	2.7067e-03
Operator Splitting	5.4037e-04	3.3764e-04	3.4641e-04
Front Kwok	8.3661e-03	4.9372e-03	1.1764e-03
Han Wu	6.0498e-04	4.7749e-04	5.1769e-04
OCA	1.1832e-04	1.6125e-04	1.1832e-04
KT	6.3875e-04	5.3292e-04	5.4037e-04

the numerical option values and Greeks of KT to corresponding reference values. KT offers good approximation of option prices and Greeks. Table 5.4 compares RMS errors of KT, which are based on values from Table 5.3, to computed reference RMS errors of numerical methods discussed in Tangman et al. (2008); all values taken correct to four decimal places. KT provides RMS errors in line with methods that are customised to price American options only, while retaining the simplicity of the "Black-Box" approach.

5.3 Barrier Option

We solve call up-and-out barrier options using KT based on the implementation described in Section 4.5. We aim to test the behaviour of KT at the sharp discontinuity appearing at the upper barrier level.

Problem 5.5 For a call up-and-out barrier option, we use the set of parameters $\sigma = 0.25$, $r = 0.10$,

Table 5.5: Accuracy for Problem 5.5.

N	L_1 Norm	L_1 Order	L_∞ Norm	L_∞ Order
10	1.3322e-01	-	6.5761e-01	-
20	3.3401e-02	1.9958	1.7558e-01	1.9051
40	8.4886e-03	1.9763	4.4154e-02	1.9916
80	2.1318e-03	1.9934	1.1065e-02	1.9965
160	5.3308e-04	1.9997	2.7723e-03	1.9969
320	1.3325e-04	2.0002	6.9138e-04	2.0035
640	3.3346e-05	1.9985	1.7201e-04	2.0070
1280	8.3620e-06	1.9956	4.2626e-05	2.0127
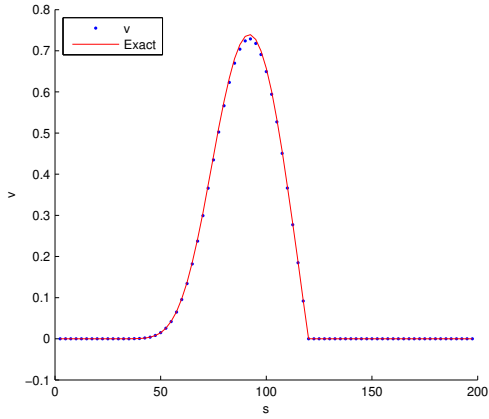
(a) Price, v
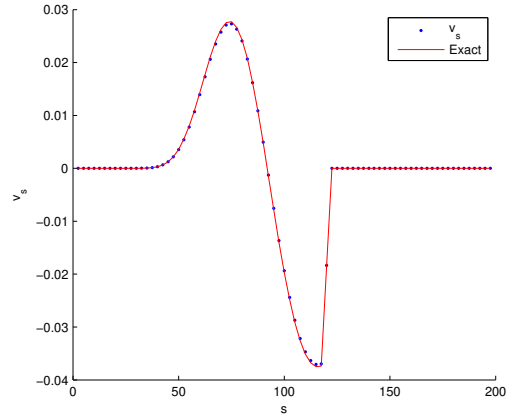
(b) Delta, v_s
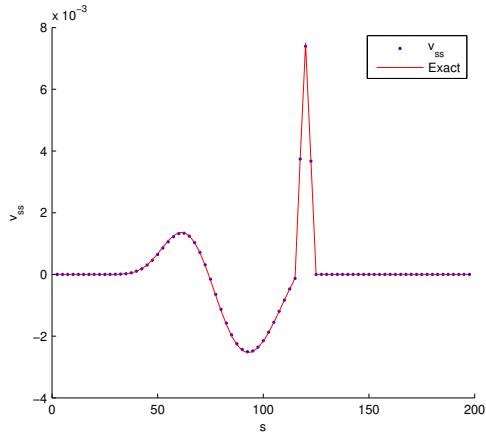
(c) Gamma, v_{ss}
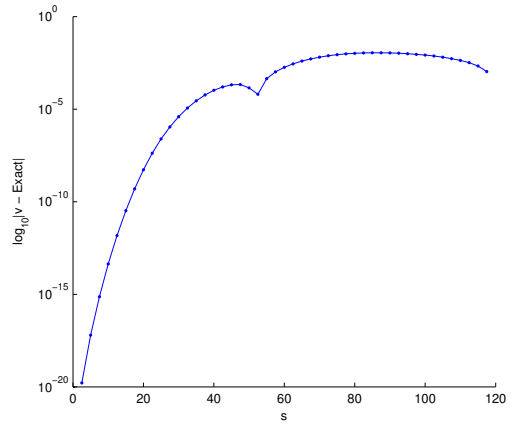
(d) Error plot

Figure 5.2: Solutions for Problem 5.5.

$\delta = 0.05$, $T = 1.00$, $K = 100$, $s \in [0, 200]$ and $B = 1.20K$, taken from Derman and Kani (1996).

Table 5.5 records the L_1 and L_∞ errors and convergence rates for Problem 5.5. For this problem, the 'first-try' ode45 solver acts inefficient by slowing down computation, therefore we switch to ode15s (Shampine and Reichelt, 1997). KT outputs very small error magnitudes and second-order convergence rate. Fig 5.2 shows the numerical solution, Greeks and error plot for Problem 5.5 using $N = 80$. KT offers non-oscillatory and high-resolution approximations even at region of discontinuity appearing in the initial profile and Greeks.

(a) Price, v

(b) Delta, v_s

(c) Gamma, v_{ss}

(d) Error plot
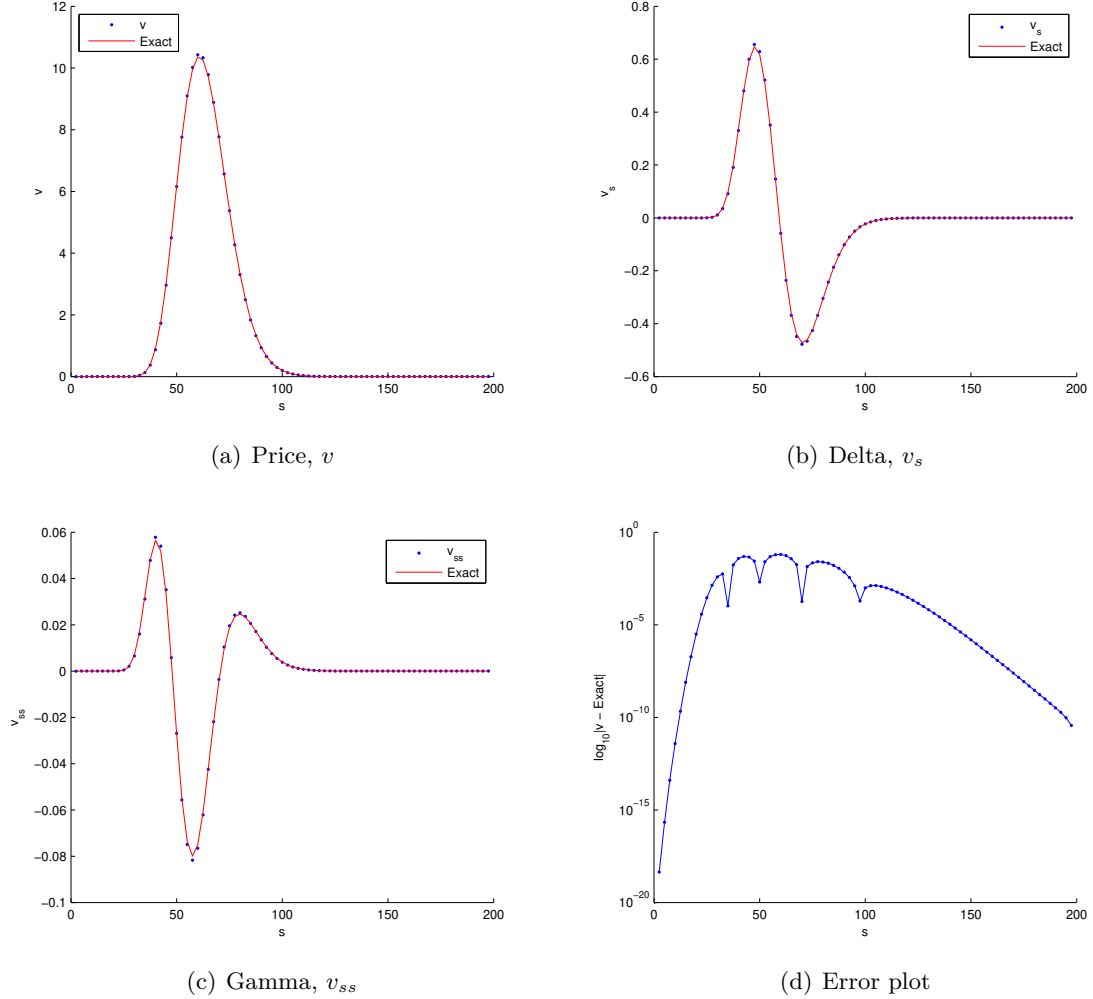
Figure 5.3: Solutions for Problem 5.6.

5.4 Butterfly Spread

We price a butterfly spread which involves buying two calls at strikes K_1 and K_3 and selling two calls at strike $K_2 = \frac{1}{2}(K_1 + K_3)$ where $K_1 < K_2 < K_3$. It tests the robustness of KT in the presence of sharp corners at strikes in the initial condition and jumps in Greeks. We apply (22) to (26) for initial function

$$v(s, 0) = \max\left(s - K_1, 0\right) + \max\left(s - K_3, 0\right) - 2\max\left(s - \frac{1}{2}\left(K_1 + K_3\right), 0\right),$$

and boundary conditions $v(s, t) = 0$ as $s \to 0$ and $v(s, t) = 0$ as $s \to \infty$.

Problem 5.6 For the butterfly spread pricing, the parameters $\sigma = 0.20$, $r = 0.10$, $\delta = 0.00$, $T = 0.50$, $K_1 = 45$, $K_3 = 80$ and $s \in [0, 200]$ are extracted from Pindza et al. (2013).

Fig 5.3 displays the numerical price, Greeks and error plot for $N = 80$. We use ode15s as ode45 acts inefficient. In line with Pindza et al. (2013), KT delivers excellent numerical results for the option price and derivatives. It guarantees oscillation-free and thus high-resolution approximations even at sharps kinks in the initial profile and multiple jumps in the derivative profiles. Also, we record the L_1 and L_∞ errors and convergence rates in Table 5.6. Despite the challenges posed by this pricing problem, KT achieves second-order convergence.

5.5 Digital Option

A cash-or-nothing digital call option has a payoff which equals either a predefined quantity after strike price or nothing at all before or at the strike threshold. We test the efficiency of KT at the sharp

15

Table 5.6: Accuracy for Problem 5.6.

N	L_1 Norm	L_1 Order	L_∞ Norm	L_∞ Order
10	2.6942e-01	-	1.4094e-00	-
20	7.3663e-02	1.8708	4.6980e-01	1.5850
40	3.0875e-02	1.2545	2.1442e-01	1.1316
80	8.0044e-03	1.9476	6.1546e-02	1.8007
160	2.1019e-03	1.9291	1.6463e-02	1.9024
320	5.3992e-04	1.9609	4.2301e-03	1.9605
640	1.3679e-04	1.9808	1.0772e-03	1.9734
1280	3.4425e-05	1.9904	2.7086e-04	1.9916

Table 5.7: Accuracy for Problem 5.7.

N	L_1 Norm	L_1 Order	L_∞ Norm	L_∞ Order
10	2.0101e-02	-	1.5876e-01	-
20	4.2580e-03	2.2390	3.5663e-02	2.1544
40	1.2339e-03	1.7869	1.0991e-02	1.6981
80	2.8435e-04	2.1175	2.3851e-03	2.2042
160	6.6769e-05	2.0904	5.4855e-04	2.1203
320	1.6001e-05	2.0610	1.3393e-04	2.0341
640	3.8951e-06	2.0384	3.2744e-05	2.0322
1280	9.6446e-07	2.0139	8.0337e-06	2.0271

discontinuity appearing in the initial profile. It suffices to effortlessly apply (22) to (26) for initial condition

$$v(s,\, 0) = \begin{cases} 1 & \text{for} \quad s \geq K, \\ 0 & \text{for} \quad s \leq K, \end{cases}$$

and subject to boundary conditions $v(s,\, t) = 0$ as $s \to 0$ and $v(s,\, t) = \exp(-rt)$ as $s \to \infty$.

Problem 5.7 We solve the digital call option with parameters taken from Pindza et al. (2013), $\sigma = 0.20$, $r = 0.10$, $\delta = 0.00$, $T = 0.50$, $K = 45$ and $s \in [0,\, 200]$.

Similar to the barrier option and butterfly spread problems, we use ode15s solver instead of ode45s. For Problem 5.7, Fig 5.4 displays the option price, Greeks and error plot for $N = 80$. KT delivers very satisfactory numerical results in line with Pindza et al. (2013). It achieves non-oscillatory and high-resolution approximations of the sharp discontinuity at the strike and resulting jumps in the Greeks. Table 5.7 records very small L_1 and L_∞ errors and second-order convergence rates despite the challenges posed by digital options.

5.6 Asian Options

We price the fixed and floating strike Asian put options from Ramírez-Espinoza and Ehrhardt (2013) by solving the two-dimensional PDE (29) using (24). This requires extending the algorithm in Section 4.3 to two spatial variables and involves matrix computations of size $(N + 1) \times (N + 1)$.

Problem 5.8 The fixed strike Asian put option is solved for $\sigma = 0.25$, $r = 0.05$, $T = 0.20$, $K = 100$, $s \in [0,\, 200]$, $a \in [0,\, 200]$ and $N = 50$ subject to conditions (30) and (31).

Problem 5.9 The floating strike Asian put option is solved for parameters $\sigma = 0.30$, $r = 0.15$, $T = 1.00$, $K = 100$, $s \in [0,\, 200]$, $a \in [0,\, 200]$ and $N = 50$ subject to conditions (30) and (32).

(a) Price, v

(b) Delta, v_s

(c) Gamma, v_{ss}

(d) Error plot
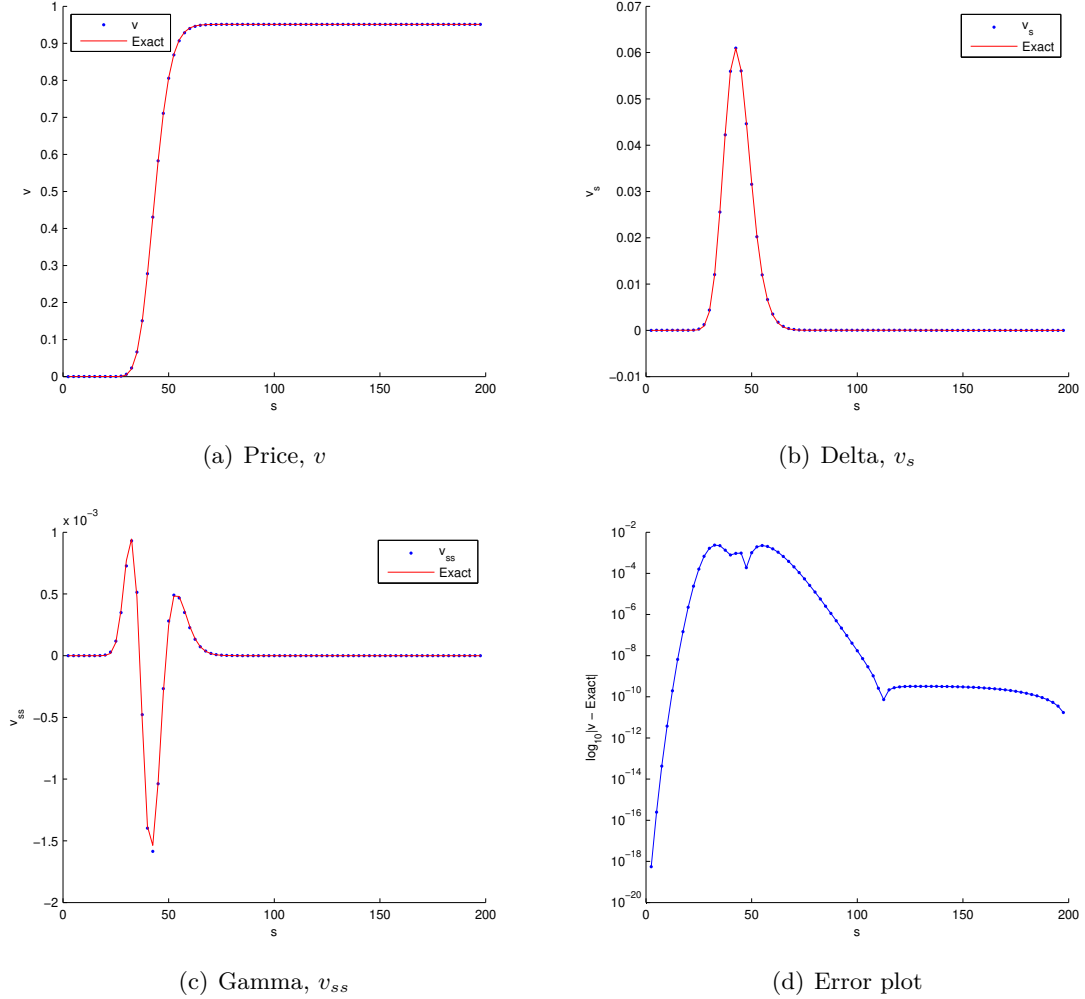
Figure 5.4: Solutions for Problem 5.7.

Table 5.8: Accuracy for Problems 5.8 and 5.9.

	Fixed strike Asian			Floating strike Asian		
N	KT	Error	Order	KT	Error	Order
10	0.8209	-	-	2.8487	-	-
20	1.5237	7.0284e-01	-	3.3864	5.3765e-01	-
40	2.1060	5.8231e-01	0.2714	3.5467	1.6032e-01	1.7457
80	2.2740	1.6801e-01	1.7932	3.5867	3.9964e-02	2.0042
160	2.3065	3.2493e-02	2.3704	3.5968	1.0140e-02	1.9787

Figs 5.5 and 5.6 show numerical solutions for Problems 5.8 and 5.9 respectively using ode45 and MM limiter (33) with $\theta = 1.5$. KT scheme offers non-oscillatory and high-resolution approximations of option value and Greeks for both fixed and floating strike cases despite the convection-dominated nature. In particular for the floating strike problem, as compared to Ramírez-Espinoza and Ehrhardt (2013), Fig 5.6 (c) shows oscillation-free approximation of Greek delta, v_s even at the $s_{\min}$ boundary. Table 5.8 shows second-order convergence rates over refined grids for both the fixed and floating strike problems. Also, we achieve a remarkable reduction in computation time from ~ 4 minutes to ~ 10 seconds for the fixed strike and from $\sim 6 - 8$ minutes to ~ 18 seconds for the floating strike as compared to results recorded in Ramírez-Espinoza (2011). This improvement is based on our fully vectorised algorithm and efficient use of time solvers. The vectorised formula (33) bypasses the loop-based formula (12), which requires high computational effort in two-dimensions. Further, we make efficient use of ode45 solver in

(a) Initial Condition, v_0

(b) Price, v

(c) Delta, v_s

(d) Gamma, v_{ss}
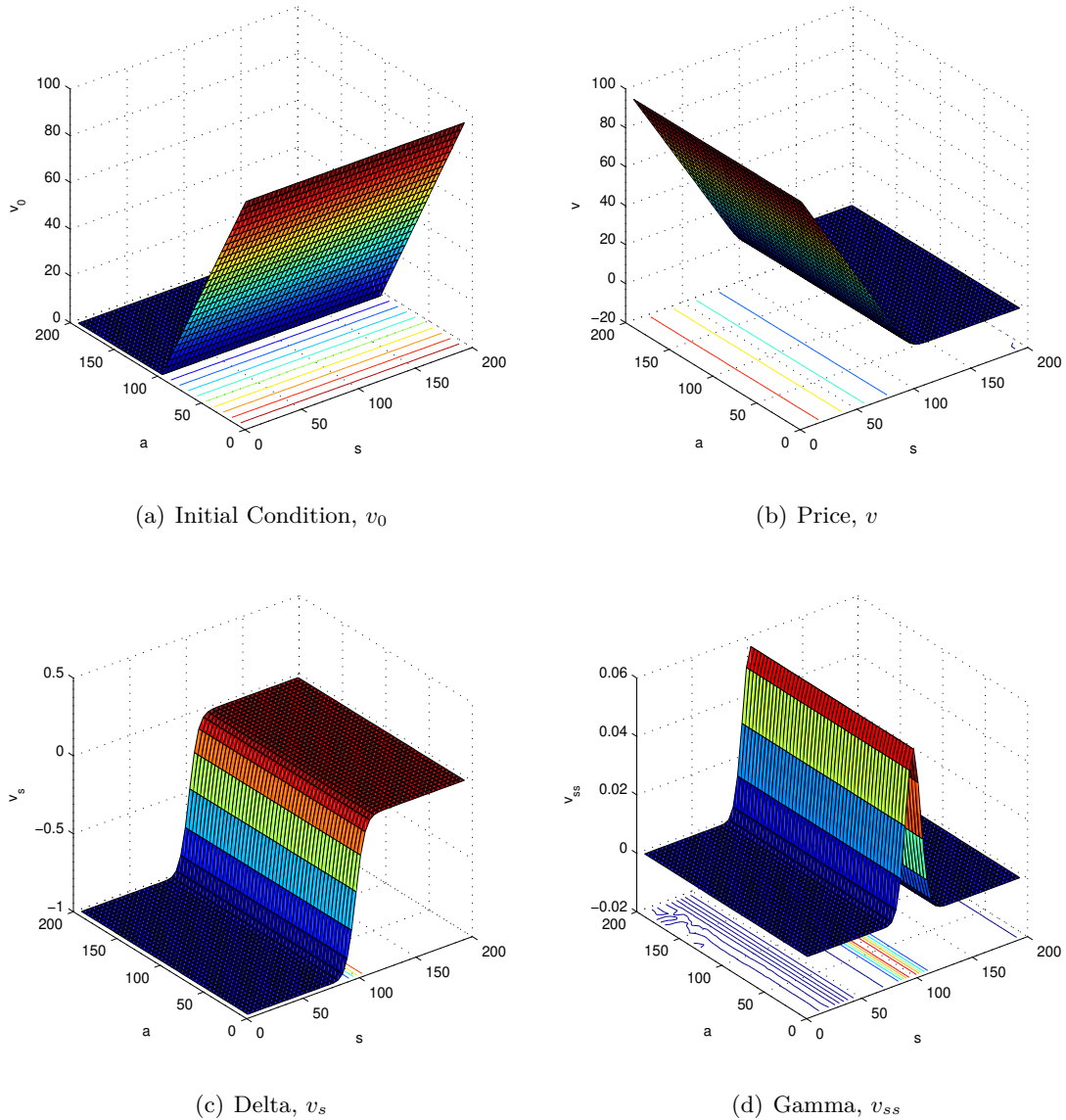
Figure 5.5: Solutions for Problem 5.8.

non-stiff environment instead of ode15s, which tends to be time-consuming in two-dimensional setup.

6 Conclusion

In this work, we have proposed an improvement of Ramírez-Espinoza and Ehrhardt (2013) approach to option pricing PDEs, formulated in the conservative form. This includes the combination of the "Black-Box" KT reconstructions with vectorised slope limiters and stable time-solvers to ensure non-oscillatory and high-resolution numerical solutions. Our fully vectorised approach and efficient use of time-solvers contribute to significant reduction in computation time. Numerical experiments are successfully performed on standard, challenging and convectively dominated European options. Also, we price barrier, butterfly and digital problems with sharp discontinuities in the initial and Greek profiles. Despite the challenges, KT offers second-order convergence as well as non-oscillatory and high-resolution numerical solutions and Greeks. Further, to the authors' knowledge, this is the first time that American and barrier options are priced by extending KT. For American options, we achieve good approximation of numerical solutions and Greeks for different sets of parameters with or without dividend. In the two-dimensional setup, as compared to Ramírez-Espinoza (2011), we obtain considerable reduction in computation time for both fixed and floating strike Asian options through our effective implementations.

(a) Initial Condition, v_0 (b) Price, v

(c) Delta, v_s (d) Gamma, v_{ss}
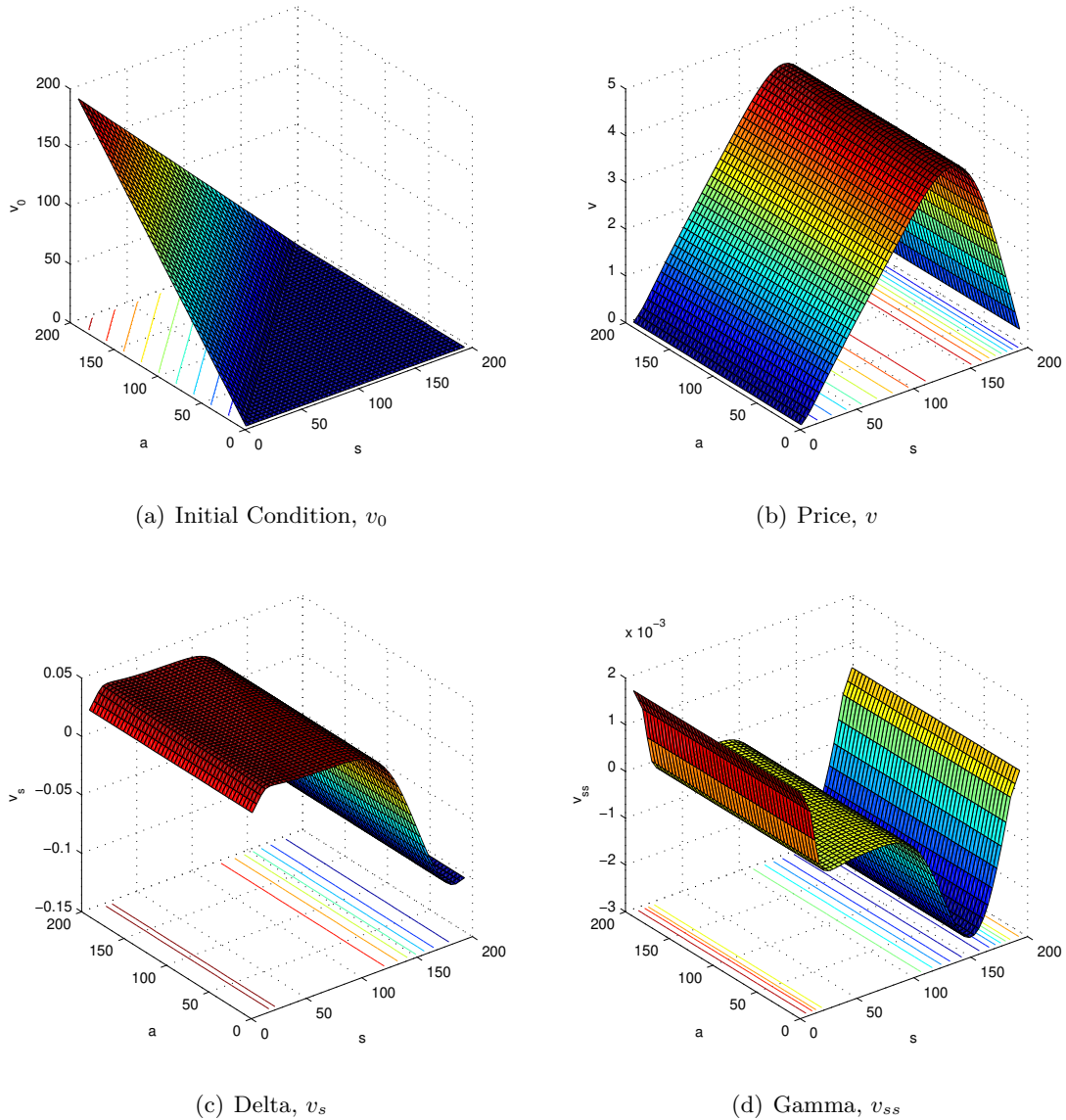
Figure 5.6: Solutions for Problem 5.9.

Declaration of interest: The authors report no conflicts of interest. The authors alone are responsible for the content and writing of the paper.

References

Barraquand, J. and Pudet, T. (1996). Pricing of American path-dependent contingent claims. *Math. Finan.*, **6**(1), 17–51. (https://doi.org/10.1111/j.1467-9965.1996.tb00111.x).

Black, F. and Scholes, M. (1973). The pricing of options and corporate liabilities. *J. Polit. Econ.*, **81**(3), 637–654. (http://dx.doi.org/10.1086/260062).

Derman, E. and Kani, I. (1996). The ins and outs of barrier options: Part 1. *Derivatives Quarterly, Winter*, pages 55–67.

Gottlieb, S., Shu, C.-W., and Tadmor, E. (2001). Strong stability-preserving high-order time discretization methods. *SIAM Rev.*, **43**(1), 89–112. (https://doi.org/10.1137/S003614450036757X).

Harten, A. and Osher, S. (1987). Uniformly high-order accurate non-oscillatory schemes. *SIAM J. Numer. Anal.*, **24**(2), 279–309. (https://doi.org/10.1137/0724022).

Kurganov, A. and Lin, C. T. (2007). On the reduction of numerical dissipation in central-upwind schemes. *Commun. Comput. Phys.*, **2**(1), 141–163.

Kurganov, A., Noelle, S., and Petrova, G. (2001). Semi-discrete central-upwind scheme for hyperbolic conservation laws and Hamilton-Jacobi equations. *SIAM J. Sci. Comput.*, **23**(3), 707–740. (https://doi.org/10.1137/S1064827500373413).

Kurganov, A. and Tadmor, E. (2000). New high-resolution central schemes for non linear conservation laws and convection-diffusion equations. *J. Comput. Phys.*, **160**(1), 241–282. (https://doi.org/10.1006/jcph.2000.6459).

Leisen, D. and Reimer, M. (1996). Binomial models for option valuation – examining and improving convergence. *Appl. Math. Fin.*, **3**(4), 319–346. (https://doi.org/10.1080/13504869600000015).

Lötstedt, P. and von Sydow, L. (2015). Numerical option pricing without oscillations using flux limiters. *Comput. Math. App.*, **70**(1), 1–10. (https://doi.org/10.1016/j.camwa.2015.04.003).

Merton, R. C. (1973). Theory of rational option pricing. *Bell. J. Econ. & Mgmt. Sci (The RAND Corporation)*, **4**(1), 141–183. (https://doi.org/10.2307/3003143).

Nessyahu, H. and Tadmor, E. (1990). Non-oscillatory central differencing for hyperbolic conservation laws. *J. Comput. Phys.*, **87**(2), 408–463. (https://doi.org/10.1016/0021-9991(90)90260-8).

Oosterlee, C. W., Frisch, J. C., and Gaspar, F. J. (2004). TVD, WENO and blended BDF discretizations for Asian options. *J. Comput. Visual. Sci.*, **6**(2-3), 131–138. (https://doi.org/10.1007/s00791-003-0117-9).

Peer, A. A. I., Gopaul, A., Dauhoo, M. Z., and Bhuruth, M. (2008). A new fourth-order non-oscillatory central scheme for hyperbolic conservation laws. *Appl. Numer. Math.*, **58**(5), 674–688. (https://doi.org/10.1016/j.apnum.2007.02.004).

Pindza, E., Patidar, K. C., and Ngounda, E. (2013). Implicit-Explicit predictor-corrector methods combined with improved spectral methods for pricing European-style vanilla and exotic options. *Electron. Trans. Numer. Anal.*, **40**, 268–293.

Ramírez-Espinoza, G. I. (2011). Conservative and finite volume methods for the pricing problem. Master's thesis, Faculty of Mathematics and Natural Science, Bergische Universität Wuppertal.

Ramírez-Espinoza, G. I. and Ehrhardt, M. (2013). Conservative and finite volume methods for the convection-dominated pricing problem. *Adv. Appl. Math. Mech.*, **5**(6), 759–790. (https://doi.org/10.1017/S2070073300001223).

Serna, S. and Marquina, A. (2004). Power ENO methods: A fifth-order accurate weighted power ENO method. *J. Comput. Phys.*, **194**(2), 632–658. (http://dx.doi.org/10.1016/j.jcp.2003.09.017).

Shampine, L. F. and Reichelt, M. W. (1997). The MATLAB ODE suite. *SIAM J. Sci. Comput.*, **18**(1), 1–22. (https://doi.org/10.1137/S1064827594276424).

Tangman, D. Y., Gopaul, A., and Bhuruth, M. (2008). A fast high-order finite difference algorithm for pricing American options. *J. Comput. Appl. Math.*, **222**(1), 17–29. (https://doi.org/10.1016/j.cam.2007.10.044).

von Sydow, L., Höök, L. J., Larsson, E., Lindström, E., Milovanović, S., Persson, J., Shcherbakov, V., Shpolyanskiy, Y., Sirén, S., Toivanen, J., Waldén, J., Wiktorsson, M., Levesley, J., Li, J., Oosterlee, C. W., Ruijter, M. J., Toropov, A., and Zhao, Y. (2015). BENCHOP The BENCHmarking project in option pricing. *Int. J. Comp. Math.*, **92**(12), 2361–2379. (https://doi.org/10.1080/00207160.2015.1072172).

Zhao, J., Davison, M., and Corless, R. M. (2007). Compact finite difference method for American option pricing. *J. Comput. Appl. Math.*, **206**(12), 306–321. (https://doi.org/10.1016/j.cam.2006.07.006).

Zvan, R., Forsyth, P. A., and Vetzal, K. R. (1998). Robust numerical methods for PDE models of Asian options. *J. Comp. Finan.*, **1**(2), 39–78. (https://doi.org/10.21314/JCF.1997.006).